Cellular/Molecular

BK Channels with β3a Subunits Generate Use-Dependent Slow Afterhyperpolarizing Currents by an Inactivation-Coupled Mechanism

Xu-Hui Zeng, G. Richard Benzinger, Xiao-Ming Xia, and Christopher J. Lingle
Department of Anesthesiology, Washington University School of Medicine, St. Louis, Missouri 63110

Large-conductance, Ca^{2+}- and voltage-activated K^+ (BK) channels are broadly expressed proteins that respond to both cellular depolarization and elevations in cytosolic Ca^{2+}. The characteristic functional properties of BK channels among different cells are determined, in part, by tissue-specific expression of auxiliary β subunits. One important functional property conferred on BK channels by β subunits is inactivation. Yet, the physiological role of BK channel inactivation remains poorly understood. Here we report that as a consequence of a specific mechanism of inactivation, BK channels containing the β3a auxiliary subunit exhibit an anomalous slowing of channel closing. This produces a net repolarizing current flux that markedly exceeds that expected if all open channels had simply closed. Because of the time dependence of inactivation, this behavior results in a Ca^{2+}-independent but time-dependent increase in a slow tail current, providing an unexpected mechanism by which use-dependent changes in slow afterhyperpolarizations might regulate electrical firing. The physiological significance of inactivation in BK channels mediated by different β subunits may therefore arise not from inactivation itself, but from the differences in the amplitude and duration of repolarizing currents arising from the β-subunit-specific energetics of recovery from inactivation.

Key words: **inactivation; BK channels; afterhyperpolarization; auxiliary subunits; excitability; gating**

Introduction

Activation of Ca^{2+}- and voltage-activated, BK-type K^+ channels is regulated by two physiological signals, membrane voltage and cytosolic Ca^{2+}. In many neurons (Shao et al., 1999; Faber and Sah, 2002) and endocrine cells (Solaro et al., 1995), the influx of Ca^{2+} through Ca^{2+} channels together with membrane depolarization promotes rapid activation of BK channels, making them well suited for a role in rapid repolarization during action potentials and in generation of brief afterhyperpolarizations. However, in many cells expressing BK channels, the specific functional role of BK channels remains poorly understood. For example, for cells with clearly identified inactivating forms of BK channel, the specific physiological role of inactivation is largely unknown. Of the four distinct β subunit family members (Orio et al., 2002), both β2 and specific N-terminal splice variants of the β3 subunit produce temporally distinct N-terminal-mediated inactivation (Wallner et al., 1999; Xia et al., 1999, 2000; Uebele et al., 2000). One potentially critical aspect of β2- and β3-mediated inactivation that may impact on its physiological roles is that, in contrast to the classical, one-step inactivation mechanism of Kv channels, BK inactivation involves a two-step mechanism (Lingle et al., 2001; Benzinger et al., 2006). Specifically, channels enter a preinactivated open state that precedes the fully inactivated conformation. Whether this represents a minor mechanistic nuance of the standard one-step inactivation scheme or contributes some important functional consequences is unknown.

For inactivation of many voltage-dependent K^+ channels, it is thought that regulation of the fractional availability of the channel population by inactivation is the central factor contributing to the physiological importance of inactivation (Hille, 2001). Thus, the availability of channels at different points in cycles of electrical activity dictates their contribution to that electrical behavior. Furthermore, differences among inactivating K^+ channels in their rates of onset and recovery from inactivation may contribute to rapid or slow use-dependent changes in cellular excitability. Yet, for inactivating K^+ currents in most cells, specific tests for the physiological impact of that inactivation process are generally lacking.

Here we describe results that suggest that, for BK channel inactivation, the ability of this inactivation mechanism to regulate tail current properties may be the physiologically important consequence of inactivation of BK channels. The present results focus on inactivation properties conferred on BK channels by the β3a subunit.

We find that the specific kinetic properties of the β3a two-step inactivation process result in a use-dependent prolongation of BK tail current during recovery from inactivation. Remarkably,

Received Feb. 19, 2007; revised March 23, 2007; accepted March 23, 2007.

This work was supported by National Institutes of Health Grants DK46564 and GM068580. G.R.B. was supported by a research fellowship from the Foundation for Anesthesia Education and Research. We thank Yefei Cai and Yimei Yue for injection, care, and maintenance of oocytes. We declare that we have no competing financial interests.

Correspondence should be addressed to Christopher J. Lingle, Department of Anesthesiology, Washington University School of Medicine, Box 8054, St. Louis, MO 63110. E-mail: clingle@morpheus.wustl.edu.

DOI:10.1523/JNEUROSCI.0758-07.2007

 0270-6474/07/274707-09$15.00/0

this prolongation results in a large enhancement of the total current flux through the tail current when compared with that resulting from open BK channels simply closing. Thus, these results show that the two-step inactivation process is a mechanism by which use-dependent slow changes in BK channel tail currents can be generated. A consequence of that is that the primary functional consequence of inactivation may arise not so much from any suppression of outward current, but in the ability to regulate tail current properties.

Materials and Methods

Constructs and mutations. The mSlo1 construct (GenBank accession number NP_034740) was as used in previous work (Xia et al., 1999, 2002). The wild-type human β3a subunit (accession number NP_852006) was generated as described previously (Xia et al., 1999). The extracellular loop of the human β3 subunit is known to produce outward rectification through rapid partial blockade of inward current (Zeng et al., 2003). For some single-channel recordings, we therefore used a mutant β subunit, D20A, in which the β3a N terminus was attached to the remainder of the β2 subunit. At +150 mV and 10 μM Ca^{2+}, the inactivation time constant (τ_i) for α + β3a is 26.6 ± 1.0 ms ($n = 5$), whereas for α + D20A, τ_i = 23.8 ± 0.9 ms ($n = 8$). At −120 mV and 10 μM, for α + β3a τ_d = 29.9 ± 0.7 ms ($n = 6$), and for α + D20A τ_d = 25.7 ± 1.3 ms ($n = 8$). Methods of expression in oocytes were as described previously (Xia et al., 1999, 2002).

Physiological recordings. All recordings used inside-out patches following procedures typically used in the laboratory (Xia et al., 2002). Both single-channel and macroscopic currents were typically filtered during acquisition at 10 kHz using a four-pole Bessel filter and digitized at 100 kHz. For display purposes, additional digital filtering of displayed single-channel traces resulted in an effective cutoff frequency of 4.47 kHz. The standard pipette/extracellular solution was as follows (in mM): 140 K-methanesulfonate, 20 KOH, 10 HEPES, 2 $MgCl_2$, pH 7.0. Solutions bathing the cytoplasmic face of the patch membrane contained 140 mM potassium methanesulfonate, 20 mM KOH, 10 mM HEPES(H^+), and one of the following: 5 mM EGTA (for nominally 0 Ca^{2+}) or 5 mM HEDTA (with Ca^{2+} added to obtain 10 μM free Ca^{2+}). Solutions were calibrated with a Ca^{2+}-sensitive electrode using commercial Ca^{2+} calibration solutions (World Precision Instruments, Sarasota, FL). Experiments were done at room temperature (~22–25°C). Salts were obtained from Sigma (St. Louis, MO). N-terminal peptides were prepared by Biomolecules Midwest (Waterloo, IL) and were C-terminal amidated and purified to at least 95%. Analysis of current recordings was accomplished either with Clampfit (Molecular Devices, Sunnyvale, CA) or with programs written in this laboratory in some cases using Scilab 3.0 (www.scilab.org). For single-channel recordings, subtraction of capacitance transients and leak current was done off-line using idealized waveforms, based on traces with null events.

Simulation of currents. Current simulations (see Fig. 5) were accomplished with the IChSim program (http://www.ifisica.uaslp.mx/~jadsc/ichsim.htm, Instituto de Física de la Universidad Autónoma de San Luis Potosí, San Luis Potosí, Mexico) and confirmed with in-house simulation software. For both standard one-step and two-step inactivation, an extra closed state in the activation pathway was included to help approximate the typical activation time course of a current. For the one-step inactivation scheme

$$C1 \underset{k_{-1}}{\overset{k_1}{\rightleftharpoons}} C2 \underset{k_{-2}}{\overset{k_2}{\rightleftharpoons}} O \underset{k_{-3}}{\overset{k_3}{\rightleftharpoons}} I,$$

rates (in s^{-1}) and voltage dependencies (z) were defined as follows: k_1 = 500 s^{-1}, z_1 = 0.5e; k_{-1} = 100 s^{-1}, z_{-1} = −0.5e; k_2 = 250 s^{-1}, z_2 = 0.5e; k_{-2} = 200 s^{-1}, z_{-2} = −0.5e; k_3 = 30 s^{-1}, z_3 = 0.1; k_{-3} = 5 s^{-1}, z_{-3} = −1.0e. For simulation of two-step inactivation

$$C1 \underset{k_{-1}}{\overset{k_1}{\rightleftharpoons}} C2 \underset{k_{-2}}{\overset{k_2}{\rightleftharpoons}} O \underset{k_{-3}}{\overset{k_3}{\rightleftharpoons}} O^* \underset{k_{-4}}{\overset{k_4}{\rightleftharpoons}} I,$$

the k_{-3} k_{-4} identical rates were used except that, in addition, $k_4 = 10^6$ s^{-1} with z_4 = 0.05e and $k_{-4} = 10^4$ s^{-1} with z_{-4} = −0.05e.

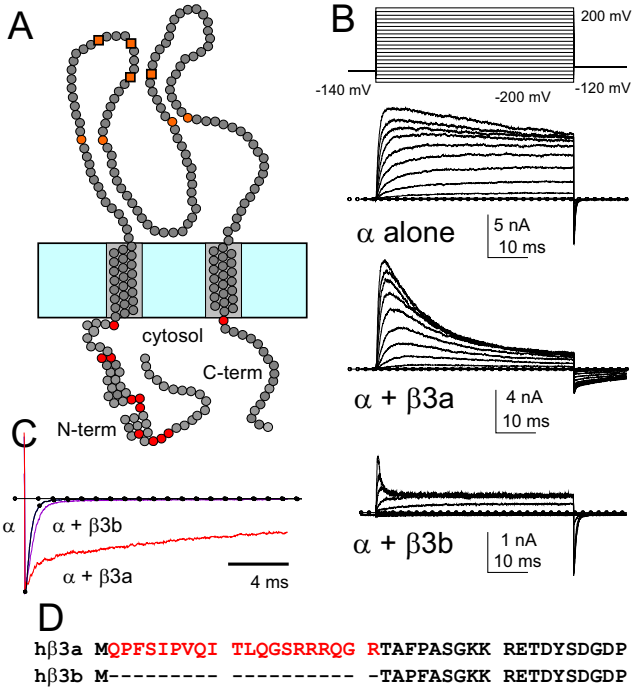

Figure 1. The N terminus of the β3a subunit mediates an inactivation-dependent slowing and enhancement of BK channel after repolarization. ***A***, BK β subunits contain two transmembrane domains joined by an extracellular loop containing sets of conserved cysteine residues (orange residues). The cytosolic N termini (N-term) of some β subunits mediate inactivation, whereas no function has been ascribed to the C terminus (C-term). The diagram shows the D20 construct, which represents a β2 subunit in which the N terminus is replaced by the β3a N terminus. Red residues on the cytosolic N terminus correspond to basic residues in the β3a N terminus. ***B***, The indicated voltage protocol was used to activate currents resulting either from α subunits alone, α + β3a subunits, or α + β3b subunits. Traces reveal the marked differences in inactivation and deactivation behavior for each type of channel. 10 μM Ca^{2+}. ***C***, Traces show the normalized tail current time course at −120 mV after depolarization to +200 mV for α alone, α + β3b, and α + β3a. ***D***, Human β3a sequence contains an additional 20 N-terminal residues compared with β3b.

Results

The β3a auxiliary subunit results in BK current inactivation and slow tail currents

BK channel auxiliary β subunits arise from four distinct genes (Orio et al., 2002) of which two, β2 (Wallner et al., 1999; Xia et al., 1999) and β3 (Uebele et al., 2000; Xia et al., 2000), encode subunits containing cytosolic N termini that confer inactivation on BK channels. For β3, four distinct splice variants have been found in the human genome, of which the β3a, b, and c variants produce inactivation (Uebele et al., 2000; Xia et al., 2000). A schematic of the β subunit putative transmembrane topology is shown in Figure 1*A*, illustrating the cytosolic orientation of the N-terminal inactivation domain and the position of charged residues in the N terminus.

Coexpression of BK pore-forming α subunits with β3a subunits results in an inactivating current (Fig. 1*B*) (τ_i ~ 25.6 ± 1.0

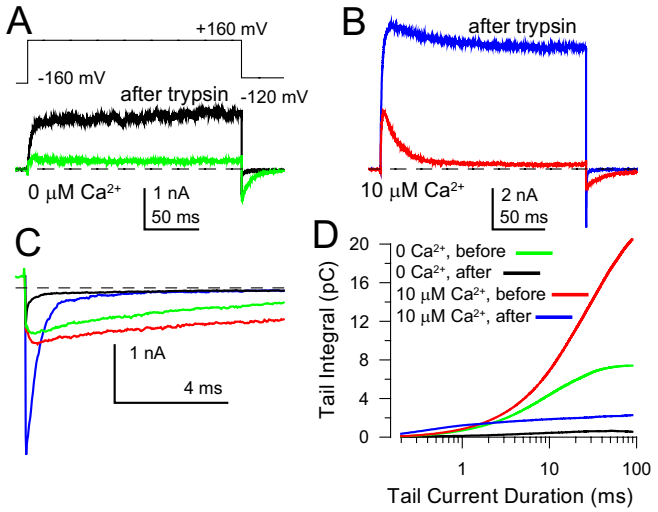

Figure 2. Removal of inactivation by cytosolic application of trypsin also abolishes slow tail current. ***A***, Removal of $\alpha + \beta$3a inactivation by cytosolic trypsin (0.1 mg/ml) abolishes tail current enhancement; 0 Ca^{2+}. ***B***, For the same patch as in ***A***, currents activated by 10 μM Ca^{2+} are shown before and after removal of inactivation by trypsin. ***C***, Expanded time base displays of tail currents at −120 mV from ***A*** and ***B*** show that removal of inactivation by trypsin speeds up deactivation time course and reduces net tail current flux. ***D***, For the tail currents in ***C***, the integral of net current through each tail currents was determined over a 100 ms time period. The net tail current flux with an intact β3a inactivation domain greatly exceeds that after removal of the inactivation mechanism.

ms at +160 mV and 10 μM Ca^{2+}; $n = 5$ patches). However, in contrast to other inactivating BK β subunits such as the β3b (Fig. 1*B*), the β3a subunit results in a marked prolongation of the tail of current during a repolarizing voltage step (Fig. 1*B*,*C*). Even at 0 μM Ca^{2+}, a condition in which open BK channels normally close very rapidly [at −60 mV, deactivation time constant (τ_d) <0.2 ms for α alone and ~1 ms for $\alpha + \beta$1 subunit (Cox and Aldrich, 2000)], there is a marked prolongation of $\alpha + \beta$3a tail current (at −60 mV, $\tau_d = 20.7 \pm 2.3$ ms; $n = 5$). As shown below, for comparable levels of current activation, the β3a subunit results in a marked increase in total current flux during a tail current compared with the α subunit alone. This prolongation of hyperpolarizing current results from a specific two-step mechanism of inactivation distinct from the standard model for inactivation mediated by cytosolic inactivation domains.

The slower-inactivating, slow-closing β3a subunit differs from the fast-inactivating, fast-deactivating β3b subunit only by an insert of an additional 20 residues at the β3a N terminus (Uebele et al., 2000) (Fig. 1*D*). This suggests that the slow deactivation may arise from the N terminus and may be related to inactivation. To test this possibility, we observed that trypsin, when briefly applied to the cytosolic face of inside-out patches, both removed inactivation and abolished the slow tail either with 0 Ca^{2+} (Fig. 2*A*) or 10 μM Ca^{2+} (Fig. 2*B*). This suggests that an intact inactivation domain is necessary for the effect of the β3a subunit on deactivation. Removal of inactivation results in a marked shortening of tail current duration (Fig. 2*C*) and a marked decrease in the net current flux through the tail current (Fig. 2*D*). In fact, with an intact β3a N terminus, the net tail current flux after activation of outward current at 0 Ca^{2+} exceeds that at 10 μM Ca^{2+}, when the N terminus has been removed by trypsin.

The development of slow tail current is coupled to the development of inactivation

We next examined the dependence of the slow tails on the development of inactivation (Fig. 3*A–C*). With brief activation steps, very few channels have inactivated, and this results in tail currents that close very rapidly. In contrast, as the command-step duration and inactivation is increased, the tail current is markedly slowed (Fig. 3*A*,*B*). In all cases, tail currents are best described by two exponential components (Fig. 3*B*). As command-step duration is increased, the percentage of slow component in the tail current increases to at least 90% (Fig. 3*C*), with little change in the individual time constants (Fig. 3*D*). That the intrinsic closing rate of the channels is not altered by the β3a subunit is supported by the fact that, after trypsin-mediated removal of inactivation, the $\alpha + \beta$3a channel closing rate is identical to the fast closing rate with an intact β3a N terminus (Fig. 3*D*). Remarkably, as inactivation develops, the total current flux during the tail currents is dramatically increased in association with the use-dependent change in tail current kinetics.

The prolongation of BK channel tail current by the β3a subunit suggests that inactivation is linked to a profound use-dependent increase in afterhyperpolarizing current. To assess the magnitude of the current enhancement produced by the β3a subunit compared with channels lacking the β3a N terminus, we determined the net tail current flux after inactivating voltage steps of different duration both at 0 Ca^{2+} (Fig. 3*E*,*F*) and at 10 μM Ca^{2+} (Fig. 3*F*). For comparison, tail current flux after removal of inactivation by trypsin was also determined. At both 0 and 10 μM Ca^{2+}, large increases in net tail current flux were observed with increases in command-step duration (up through 200 ms). When the β3a inactivation structure was cleaved by trypsin, only modest increases in tail current flux were observed with increases in command-step duration (longer than 5 ms). The tail current integral after a 200 ms activation step at 0 Ca^{2+} with an intact β3a N terminus was 2.69 ± 0.45-fold ($n = 6$ patches) greater than the tail current integral at 10 μM Ca^{2+} after removal of inactivation by trypsin. Thus, slow entry into inactivated states mediated by the β3a N terminus results in a use-dependent increase in the net tail current flux. The total tail current flux greatly exceeds that which would be observed without a β subunit, as indicated by the effect of trypsin.

Trains of brief depolarizations elicit a use-dependent development of $\alpha + \beta$3a persistent tail current

To test whether normal cellular electrical activity might produce such a use-dependent increase in tail current, we used command protocols in which channels were activated by brief (3 ms) repetitive (120 Hz) steps to +80 mV, to approximate high-frequency electrical firing (Fig. 4). Under such conditions, with 10 μM Ca^{2+}, $\alpha + \beta$3a current shows a gradual reduction in the outward current activated at +80 mV as channels accumulate in inactivated states (Fig. 4*A*,*C*). Furthermore, although the peak of the initial tail current gradually decreases, the level of tail current at the end of each hyperpolarizing step gradually increases with pulse number (Fig. 4*A*,*D*). In contrast, after disruption of inactivation with trypsin, there are no use-dependent changes either in outward current or tail current (Fig. 4*B–D*). This indicates that, with brief, high-frequency stimulation, $\alpha + \beta$3a channels can mediate use-dependent changes in slow afterhyperpolarizing current. Because $\alpha + \beta$3a inactivation is not Ca^{2+} dependent, and the prolongation of slow tails is observed in 0 Ca^{2+}, the slow tail has the characteristics suitable for mediating a use-dependent but Ca^{2+}-independent slow afterhyperpolarization.

Enhancement of net tail current flux can arise from a two-step inactivation mechanism

The β3a tail current prolongation depends on an intact inactivation mechanism. Yet the simplest model of inactivation ($C \leftarrow O \rightleftharpoons I$) in which inactivated channels simply pass back through a single type of open state cannot result in a net current flux that exceeds that resulting from normal channel closing (Demo and Yellen, 1991). Both the BK β2 and β3b subunits produce inactivation by a two-step mechanism (Lingle et al., 2001; Benzinger et al., 2006) in which channels first enter a preinactivated open state before complete inactivation ($C \leftarrow O \rightleftharpoons O^* \rightleftharpoons I$).

Using protocols to examine use-dependent changes in instantaneous current properties of α + β3a currents, we established that α + β3a currents also exhibit the hallmarks of two-step inactivation (supplemental Fig. 1, available at www.jneurosci.org as supplemental material).

During recovery from inactivation, β2 and β3b channels differ in the extent to which inactivated channels can return to closed states without passing through a fully open state (Lingle et al., 2001; Benzinger et al., 2006). It therefore seemed possible that perhaps the unique characteristic of α + β3a currents responsible for the tail current enhancement is that, in contrast to inactivation mediated by α + β2 channels, recovery from inactivation may be obligatorily coupled to passage back through the fully open state. To assess the potential impact of a two-step inactivation mechanism in which recovery involves obligatory passage through open states, we therefore compared simulations of tail currents arising either from the simple, one-step inactivation mechanism (Fig. 5*A*,*B*) or the two-step mechanism (Fig. 5*C*,*D*). These comparisons showed that a two-step mechanism, in which recovery from inactivation requires passage back through the open state, can readily generate net tail current flux that far exceeds that resulting from a population of open channels simply closing. For a one-step inactivation scheme (Fig. 5*A*,*B*), the tail current integral after development of inactivation is essentially identical to that expected for all open channels simply closing (Fig. 5*B*). The small discrepancy shown in the figure arises, because the brief depolarizing step was insufficient to maximally activate the population of channels. In contrast, with a two-step inactivation mechanism (Fig. 5*C*,*D*), recovery from inactivation is associated with marked enhancement of net tail current flux.

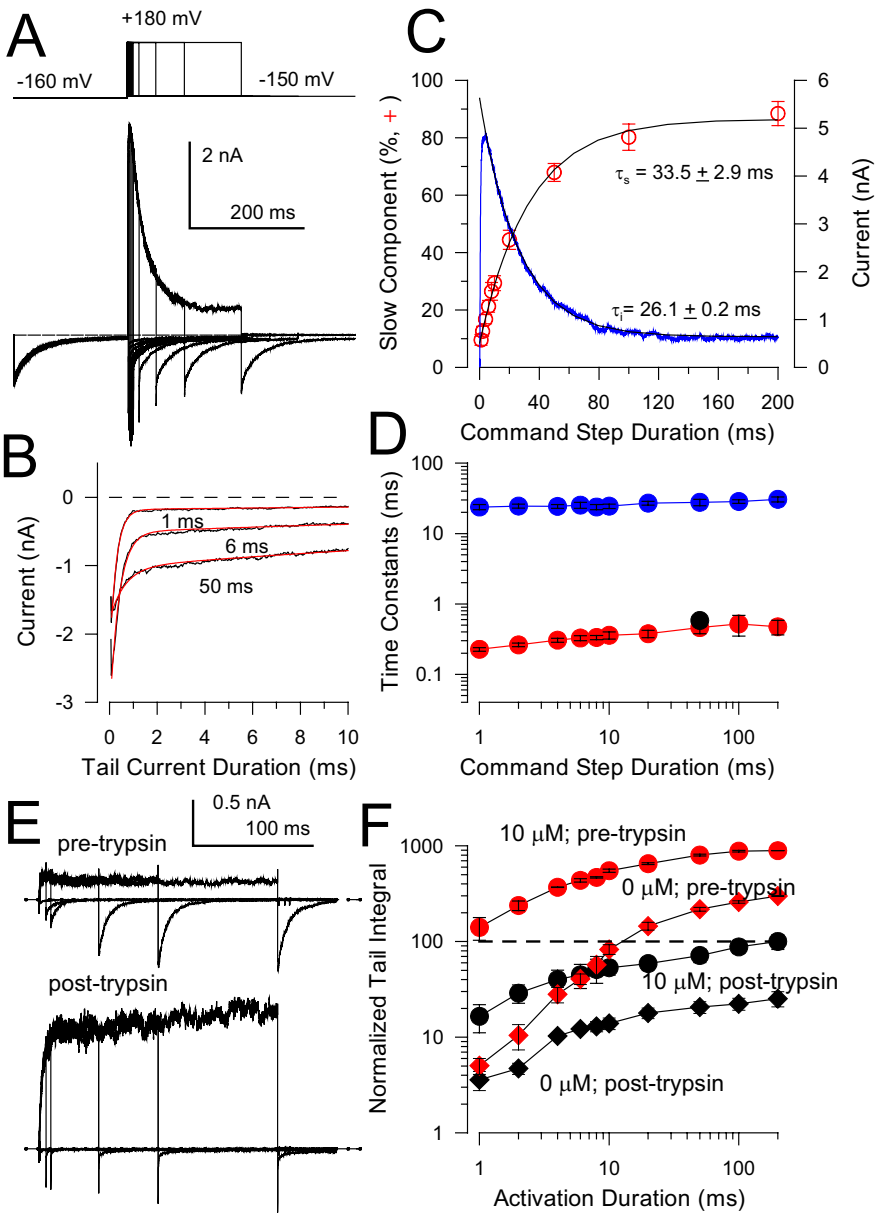

Figure 3. Inactivation of α + β3a currents is coupled to the use-dependent increase in net tail current flux. ***A***, α + β3a currents were activated by the indicated protocol with 10 μM cytosolic Ca^{2+} to allow examination of the tail current properties as a function of the duration of the preceding depolarizing voltage step. Shorter-duration depolarizing steps are associated with faster-deactivating tail currents. ***B***, The tail current decay time course (black lines) after repolarization to −150 mV was fit with a two-component exponential function (red lines) yielding a fast (τ_f) and slow (τ_s) time constant of deactivation. τ_f and τ_s were, after the 1 ms step, 0.27 ± 0.001 and 29.05 ± 0.02 ms; after the 6 ms step, 0.36 ± 0.002 and 30.23 ± 0.01 ms; and after the 50 ms step, 0.64 ± 0.01 and 32.4 ± 0.04 ms. ***C***, The time course of current inactivation (blue line) during a step to +180 mV is compared with the fractional increase in the slow component of tail current (red circles) after command steps to +180 mV of differing durations. The fitted inactivation time constant (black line) was 26.1 ± 0.2 ms. For a set of patches, the percentage of the slow component in the tail current increased as a function of command-step duration with a time constant of 33.5 ± 2.9 ms. ***D***, The time constants for τ_f and τ_s exhibit little change with command-step duration. Solid black symbol at 50 ms step duration corresponds to single exponential deactivation time after removal of inactivation by trypsin. ***E***, Changes in α + β3a tail current properties before and after removal of inactivation by trypsin are shown for 0 Ca^{2+}. The command step was to +180 mV with the tail current at −150 mV. ***F***, Tail current integrals after command steps of different durations from traces as in ***E*** were determined. In each case, net flux was normalized to that observed after a 200 ms activation step with 10 μM Ca^{2+} after removal of inactivation by trypsin. An intact β3a N terminus results in inactivation-dependent increases in net tail current flux compared with channels in which the inactivation domain is removed by trypsin.

Reopenings of single α + β3a channels during repolarization support the two-step behavior

These two distinct mechanisms of inactivation would be expected to generate quite different single-channel behaviors during re-

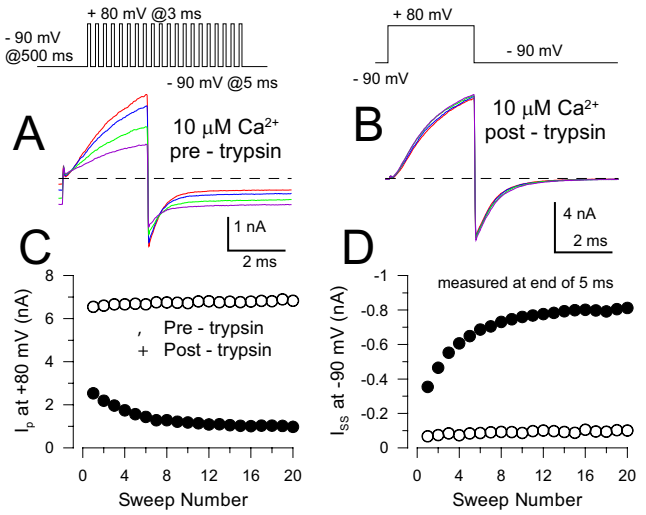

Figure 4. Brief, high-frequency depolarizations elicit development of the $\alpha + \beta$3a-mediated slow component of BK tail current. An inside-out patch was stimulated with a high-frequency train of 20 3 ms depolarizations to +80 mV (left protocol shown on top) with the protocol for each cycle of depolarization shown on the right. ***A***, The repetitive stimulation protocol results in use-dependent increase in slow $\alpha + \beta$3a tail current. An inside-out patch was stimulated repetitively, as shown, while bathed with 10 μM Ca^{2+}. Traces show a use-dependent decrease in outward current, but an increase in inward tail current at the end of each hyperpolarization to −90 mV. Traces show 1st, 2nd, 5th, and 15th of 20. ***B***, Brief trypsin application (0.5 mg/ml) removes the use-dependent changes in BK current. ***C***, Changes in peak outward current are plotted as a function of stimulus number for the experiments in ***A*** and ***B***, showing a use-dependent reduction in outward current that is removed by trypsin. ***D***, Changes in amplitude of the tail current measured at 5 ms are plotted as a function of stimulus number from the experiments in ***A*** and ***B*** showing the use-dependent enhancement of persistent tail current, which is abolished by trypsin.

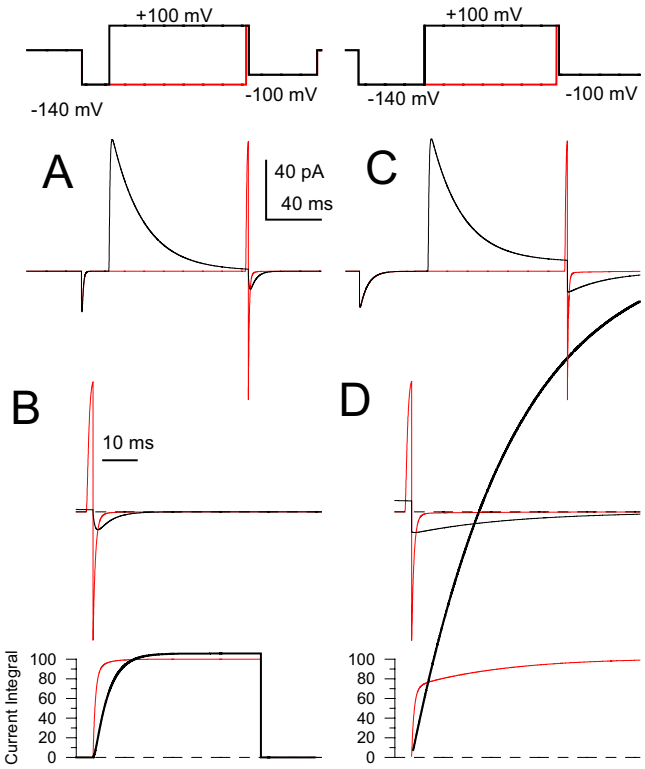

Figure 5. Two-step inactivation provides a mechanism that can generate use-dependent enhancement of net tail current flux. ***A***, Currents were simulated for a simple block model ($C1 \rightleftharpoons C2 \rightleftharpoons O \rightleftharpoons I$) with the indicated voltage protocol. Rates are given in the Materials and Methods. The longer depolarization produces current inactivation, whereas repolarization exhibits unblocking behavior characteristic of passage back through the open state. ***B***, Tail currents from the simulation in ***A*** are shown at higher time resolution (top). On the bottom, the tail current integral was determined for both traces on the top and normalized to the maximum value associated with the brief depolarization. The small excess of net tail current flux after the prolonged depolarization reflects the fact that the brief depolarization was too short to produce maximal channel activation. ***C***, Using the indicated stimulation protocol, currents were simulated with a two-step inactivation model ($C1 \rightleftharpoons C2 \rightleftharpoons O \rightleftharpoons O^* \rightleftharpoons I$) with rates given in the Materials and Methods. ***D***, Tail currents from the simulation in ***C*** shown at a faster time base (top) emphasize the marked prolongation of tail current decay, whereas the tail current integrals (normalized to values in ***B***) show the marked enhancement of net tail current flux associated with recovery via a two-step inactivation pathway.

covery from inactivation. For classical, one-step inactivation, recovery from inactivation will be associated with a brief period in the blocked state, before an opening to a full conductance level and then closing. For two-step inactivation, dependent on the kinetics of the O^*-I equilibrium, we would expect that after repolarization, a channel might immediately reopen to a conductance level reflecting the new O^*-I equilibrium. In accordance with the two-step scheme, the duration of the O^*-I burst should be the underlying determinant of the slow tail currents.

To test this idea, we examined properties of $\alpha + \beta$3a single channels during depolarizations and after repolarization. For these experiments, we used a D20A construct (see Materials and Methods), in which the human β3a N terminus replaces the N terminus of the β2 subunit. Brief depolarizing steps to +150 mV with 10 μM Ca^{2+} were used to activate a single BK channel (Fig. 6). At the end of the 10 ms depolarization, channels either remained open (Fig. 6*A*) or had inactivated (Fig. 6*B*). Dependent on whether the channel was open or had inactivated, the resulting behavior after depolarization was markedly different. When the channel had not inactivated, a typical brief BK channel tail opening is observed (Fig. 6*A*). In contrast, for a channel that had inactivated during the depolarization (Fig. 6*B*), that channel immediately reopens to a prolonged burst with a flickery current level of reduced conductance. Separately grouping tail current openings dependent on whether the channel was open or closed at the end of the depolarization directly shows that the fast component of deactivation in macroscopic $\alpha + \beta$3a tails reflects normal channel closing (Fig. 6*A*), whereas the slow tails specifically reflect the inactivation-dependent closures (Fig. 6*B*,*C*). Intriguingly, for many of the prolonged tail current single-channel openings, the tail current burst terminates with a brief excursion to a larger current level (Fig. 6*B*, black arrows). The average of all tail current openings generates a current that only partially inactivates within 10 ms and shows both the fast and slow component of tail current consistent with the macroscopic measurements. For command-step durations of 150 ms, essentially all openings after repolarization were of long duration and reduced conductance (data not shown).

Table 1 summarizes the statistical occurrence of different categories of event combination for 1471 records from five patches examined with the same stimulation conditions. For all cases in which the channel is open at the end of the depolarizing step (n = 404), 87.4% of the time a normal tail opening was observed, whereas 9.9% of the time, no opening was detectable (in part because of the limited time resolution of the recording). For 11 of 404 cases, an O^*-I burst was observed in the tail, but for almost all of these cases, it appeared that there was initially a brief transition at the O level. For all cases in which a channel inactivated during the depolarizing step (n = 607), after repolarization, the channel immediately entered an O^*-I burst 71.8% of the time but entered O 3.5% of the time. In 105 of 607 cases (24.7%), no tail opening

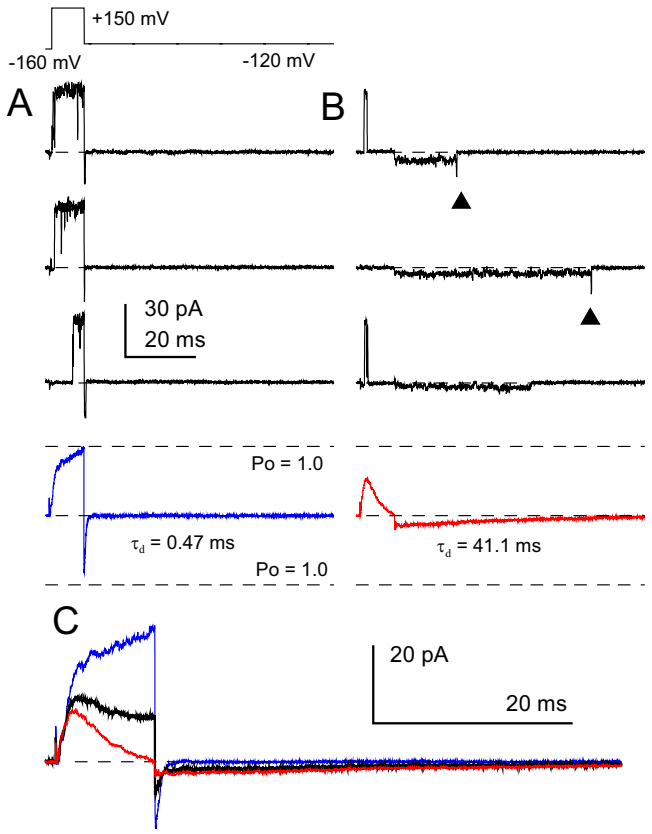

Figure 6. The β3a inactivation particle produces prolonged low-conductance bursts. A 10 ms depolarization with 10 μM Ca^{2+} was used to activate openings of a single BK (α + D20A) channel, and all traces in ***A*** and ***B*** are from the same patch. ***A***, Three examples in which the channel was open at the end of the 10 ms step are shown, and, on the bottom, the ensemble average (blue trace) plotted in units of open probability (Po) is displayed for all such sweeps in this patch. The averaged tail current decayed with a τ_d of 0.47 ms. ***B***, Sweeps are shown in which the channel inactivates either before or during the 10 ms step resulting in a prolonged, low-amplitude tail current opening. The diamonds indicate larger-conductance openings that often terminate the prolonged bursts. On the bottom (red trace), the ensemble average for traces in which the channel was inactivated before repolarization is shown. The tail current decayed with a time constant of 41.1 ms. ***C***, Traces show the averages for all sweeps (black), sweeps with no inactivation (blue), and those sweeps with inactivation (red). For the brief 10 ms depolarization, the ensemble tail current of all openings contains both fast and slow deactivating components, whereas the tail current for channels that were inactivated before depolarization shows only slow deactivation.

was observed, which greatly exceeds the 9.9% of the time that tail openings are not detected when a channel is open at the end of a preceding depolarization. Thus, although the occurrence of the O^*-*I* bursts clearly is the predominant event as a channel recovers from inactivation, the results reveal the occurrence of a direct closed-state pathway to recovery. More detailed analysis of such records will be presented elsewhere.

As a first approximation, this single-channel behavior can be explained within the context of the two-step inactivation scheme, also observed in other BK β subunits (Lingle et al., 2001; Benzinger et al., 2006), in which formation of the inactivated state (*I*) occurs subsequent to a preinactivated open state ($C \leftarrow O \rightleftharpoons O^* \rightleftharpoons I$). At positive potentials, the O^*-*I* equilibrium strongly favors *I*, such that no O^* openings are observed. However, after repolarization, inactivated channels then oscillate rapidly between O^* and *I*, resulting in an apparent single-channel current level less than a full open level. For the β2 subunit, the current level of the O^* state is indistinguishable from that of the *O* state (Benzinger et al., 2006); thus, we consider it likely that the

Table 1. Pairings of event classes

Summary of event classes and event occurrences	Total events ($n = 5$ patches)	*p* (event class)
O2∩*O1*	353	0.239973
O2∩*I1*	21	0.014276
O2∩*C1*	1	0.00068
(*O*-I*)*2*∩*O1*	11	0.007478
(*O*-I*)*2*∩*I1*	436	0.296397
(*O*-I*)*2*∩*C1*	250	0.169952
C2∩*O1*	40	0.027192
C2∩*I1*	150	0.101971
C2∩*C1*	209	0.14208
Total traces (from 5 patches)	1471	1.0
Total *O1*	404	0.274643
Total *I1*	607	0.412644
Total *C1*	460	0.312712
Total (*O1* and *I1*)	1011	0.6872
Total (*O*-I*)*2*	726	0.473827
Total *O2*	375	0.254929
Total *C2*	399	0.271244

Single-channel patches were activated by a 10 ms depolarization to +150 mV (pulse 1) with 10 μM Ca^{2+} after a 40 ms step to −160 mV. Tail events were monitored at −120 mV (pulse 2). *X2*∩*Y1* denotes those occurrences where event *X* during pulse 2 followed event *Y* during pulse 1. *O1*, During pulse 1, the channel opened and remained open at the end of the step. *I1*, During pulse 1, the channel opened and was then closed at the end of the step. *C1*, During pulse 1, no opening was observed. *O2*, In pulse 2, the channel immediately opened to a full-conductance level. *O*-I*, In pulse 2, the channel either immediately opened to a full-conductance level, or (very rarely) an initial *O2* opening preceded an *O*-I* burst. *C2*, No opening was detectable during pulse 2.

O^* state for β3a may exhibit a similar full conductance. For β3a channels, to return to the resting condition, channels must briefly transit through state *O*, resulting in the larger current level at the end of the burst. The distinction between inactivation mediated by the β3a subunit compared with other BK β subunits is that recovery from the inactivated state appears to be more strongly coupled to passage through the open state. However, the appreciable occurrence of tail events in which no opening is observed (Table 1) indicates that coupling of recovery to passage through open states is not obligatory. An intriguing implication of this mechanism is that the β3a N terminus can apparently very briefly bind to a position presumably within the channel pore, which permits ion permeation but prevents channel closure, possibly reflecting a larger size of the BK central cavity than found in other K^+ channels (Wilkens and Aldrich, 2006).

β subunit N-terminal peptides mimic the specific effects of intact β subunits on modulation of BK tail current properties

To confirm the key role of the β3a N terminus in two-step inactivation and tail current prolongation, we tested the ability of a peptide corresponding to the first 20 residues of the β3a N terminus to mimic the behavior of the full subunit (Fig. 7). Application of 10 μM β3a(1–20) peptide to a single-channel patch expressing solely BK α subunits produced both a prolonged blocked state at positive potentials and also the unique tail current openings characteristic of the intact β3a subunit. Specifically, reopening to a prolonged level of reduced conductance occurs immediately after repolarization. Such bursts are generally terminated by a brief opening to a full conductance level. Thus, qualitatively, the isolated β3a(1–20) peptide mimics all of the key mechanistic nuances of the intact subunit and is sufficient to produce two-step inactivation.

We next compared the ability of different BK β subunit peptides to block BK channels (Fig. 8*A*) and influence tail current flux (Fig. 8*B*,*C*). Because the peptides were each applied to the same inside-out patch, this allowed a direct comparison of the relative abilities of each N terminus to influence tail current be-

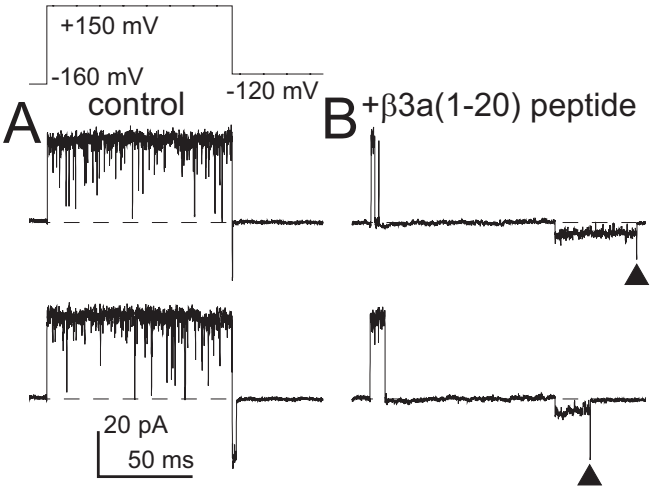

Figure 7. A β3a N-terminal peptide produces block and tail current openings characteristic of the tethered native N terminus. ***A***, A single BK channel (α subunits alone) was activated by a depolarizing step to +150 mV (as indicated) with 10 μM Ca^{2+}. Channel opening persists for the duration of the command step, but after repolarization to −120 mV, the channel rapidly closes. ***B***, Application of 10 μM β3a(1–20) peptide produces rapid and strong block during the depolarizing step. After repolarization, the channel immediately returns to a prolonged open level of reduced amplitude, with the tail opening terminated by a brief opening to a full conductance level (arrows).

havior. Similar to their parent subunits, β3b peptide produces fast and incomplete inactivation and fast deactivation (Xia et al., 2000; Lingle et al., 2001), whereas a β2 peptide produces slower and more complete inactivation with little reopening after repolarization (Xia et al., 1999). Direct comparison of the tail currents (Fig. 8*B*) shows that, whereas the β2 peptide markedly reduces tail current amplitude and net tail current flux, the β3a peptide increases net tail current flux. We measured the net tail current flux in the presence and absence of each of the three peptides after command steps varying from 1 ms through 200 ms (Fig. 8*C*). The net tail current flux for the β3b peptide as a function of command-step duration was comparable with BK α alone, showing little change for command steps >10 ms. In contrast, the β2 peptide results in a marked decrease in net tail current flux, whereas the β3a peptide produces a profound increase in net tail current flux.

To account for the differential modulation of net tail current flux within the framework of the two-step inactivation model requires that the preferential pathways for recovery from inactivation must be distinct for each β subunit, as summarized in Figure 8*D*. Our current results do not provide an explanation for how this mechanistic difference might arise.

Discussion

The results show that the β3a auxiliary subunit of BK channels confers an inactivation-dependent, slowly developing slow component of BK tail current. The development of this slow tail is dependent on a functional β3a inactivation domain, and the time course of development of the slow tail tracks the development of inactivation. Sufficient inactivation occurs even at 0 Ca^{2+} that the β3a subunit produces slow BK tail currents even in the absence of Ca^{2+}. Furthermore, brief high-frequency trains of depolarizations effectively increase the slow tail current. The results also show that the inactivation-dependent slow tail current arises as a consequence of a two-step mechanism of inactivation, characteristic of BK β subunits. Single-channel properties during tail currents exhibit features specifically predicted by the two-step scheme and that directly reveal the molecular events that underlie the tail current prolongations. Together, the results suggest that a major role of inactivation mediated by BK β subunits may lie in use-dependent modulation of BK tail current.

These results establish a mechanism by which a voltage-dependent K^+ channel, in this case a BK channel, can produce use-dependent changes in afterhyperpolarizing currents. In a real cell, a slow increase in a tail current resulting from activity of a BK channel would typically be attributed to cytosolic Ca^{2+} accumulation. In the case of α + β3a currents, although the channels mediating this effect are themselves Ca^{2+} dependent, the underlying prolongation of tail currents is Ca^{2+} independent. Most notably, the use-dependent changes in tail currents can occur in the complete absence of Ca^{2+}. Thus, α + β3a currents mediate a Ca^{2+}-independent, use-dependent prolongation of tail current with characteristics suitable to play a significant role in use-dependent changes in cellular excitability.

The key mechanism necessary to produce the slow tail currents is two-step inactivation. Rather than being a mechanistic subtlety of a particular fast-inactivation mechanism, the two-step inactivation process provides a potentially physiologically powerful mechanism by which net current during deactivation can be substantially boosted compared with the normal channel closing process. Qualitatively, tail currents after α + β3a inactivation share some similarities with resurgent current arising from particular Na^+ channels (Raman and Bean, 2001; Grieco et al., 2005); both result in a tail current slower than expected for open channels simply closing, and both depend on a specific inactivation mechanism. However, the underlying mechanism differs substantially in each case. For resurgent Na^+ channel tail current, the temporal characteristics of the tail currents are defined by the dissociation kinetics of an inactivation particle in accordance with simple block behavior, with the total current flux defined by the lifetime of open Na^+ channels. For α + β3a BK channels, the tail current duration is determined by the lifetime of the O^*-I equilibrium, which may also be defined by a dissociation event. However, the net tail current flux represents the sum of all excursions to the preinactivated state during the O^*-I burst, along with brief transitions through the fully open state before closure. The remarkable feature of the α + β3a tail currents is the large use-dependent enhancement of tail current flux compared with tail currents resulting from simple dissociation of an inactivation particle. When α + β3a tail currents are compared with tail currents arising from other inactivating BK β subunits (Xia et al., 1999; Lingle et al., 2001), the importance of blockade of the BK channel by different N termini may rest not so much with inactivation itself, but with the ability to differentially regulate properties of BK tail currents.

In native cells, there is little information about the physiological roles of inactivating BK channels. Although a potential role of BK inactivation in spike broadening in lateral amygdala has been reported previously (Faber and Sah, 2002), the specific inactivation properties of BK channels in these cells are undescribed. Furthermore, frequency dependence in the net Ca^{2+} influx per action potential might generate use-dependent changes in the contribution of BK currents to repolarization that are unrelated to inactivation. For inactivating BK channels found in rat adrenal chromaffin cells most likely containing β2 subunits (Solaro et al., 1995; Xia et al., 1999), the specific consequence of that inactivation has not been determined. For β3 subunits, Northern blots on human cDNA provide the only information on potential loci of β3 expression (Uebele et al., 2000). Although weak signals are observed in brain and strong signals in pancreas, as yet no cur-

rents in native cells have been recorded that have properties characteristic of any of the β3 splice variants. Although the Ca^{2+}-independent prolongation of the α + β3a currents described here might make them mistaken for non-BK types of currents, the signature properties of the α + β3a currents established here should help make them readily identifiable once they are encountered.

Given the potential importance of two-step inactivation as a general mechanism by which tail currents can be modulated, a critical question concerns the basis for the differences among the different β subunits. For β2, there is little or no detectable tail current during recovery from inactivation (Xia et al., 1999), whereas for β3a, the tail current is markedly enhanced. We hypothesize that both β2 and β3 N termini must interact with the α subunit in a similar type of manner. Specifically, it seems unlikely that two distinct N-terminal domains would each produce a two-step mechanism of inactivation while acting at different sites. The possibility that the phenomenon of two-step inactivation is independent of the identity of the β subunit N termini and only dependent on some unique structural characteristic of the α subunit also seems unlikely. In this regards, we know that other peptides, including the Shaker B N-terminal inactivation particle, block BK channels in a manner consistent with standard one-step inactivation (X. Zhang and C. J. Lingle, unpublished observations). Thus, two-step inactivation is specific to particular structural determinants in the N termini. How is it then that, although all of the BK inactivating β subunits show behavior consistent with a basic two-step mechanism, there are such marked differences in the pathways for recovery from inactivation? How is it that recovery from inactivation of α + β3a channels is strongly coupled to passage through a normal open state, whereas, for α + β2 channels, channels can recover while still apparently blocked by the β subunit? One hypothesis is that each type of β subunit N terminus, through slightly different specific interactions with positions on the wall of the BK central cavity, differentially influence the channel open to closed equilibrium. To test such a suggestion will require specific information both about the points of interaction between the β subunit N termini and the α subunit and also about the architecture of the BK channel central cavity. An interesting general implication of this sort of mechanism is that the relevant binding site in the BK central cavity potentially offers a site by which either endogenous or exogenous agents might modulate BK channel function.

The present results allow only limited comment regarding the physical basis of the two-step inactivation mechanism. However, we prefer the view that the binding site for the β3a N terminus, while in the preinactivated state, almost certainly resides at some position within the BK central cavity, whereas block involves occlusion of the permeation pathway at a position very close to the beginning of the cytosolic end of the selectivity filter. Because the *O*-I* current amplitude and variance directly reflect both the rates and equilibrium of the *O*-I* transitions, to account for the properties of the *O*-I* bursts, the rates of that equilibrium must be well in excess of 10^6 s^{-1}. This seems most easy to explain by assuming that any movement that accounts for the transition between *O** and *I* must be very small and is probably inconsistent with motions involving translocation of an inactivation domain from a position outside the central cavity to a pore-blocking position near the selectivity filter. This interpretation would therefore require that, while the N terminus is within the central cavity in a preinactivated conformation, ion flux is still permitted. This idea contrasts markedly with standard conceptions based on models of central cavity occupancy of Kcsa and Kv channels by quaternary blockers and peptides (Zhou et al., 2001; Faraldo-

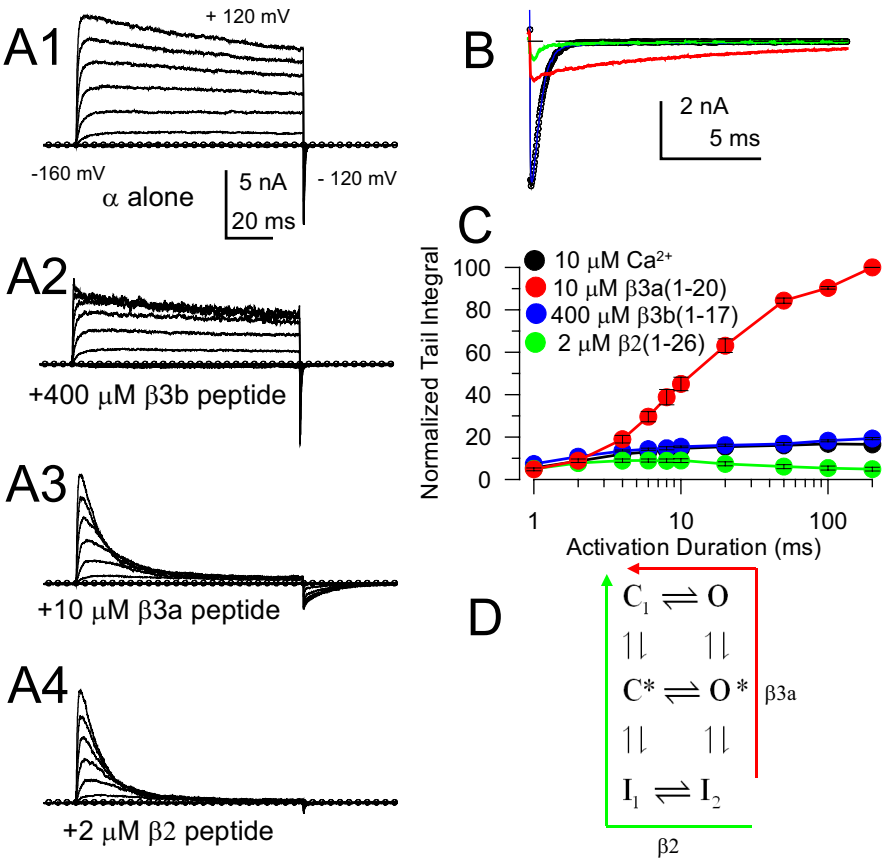

Figure 8. Distinct β subunit inactivation domains differentially regulate BK channel deactivation properties. ***A1***, The top traces show currents resulting from BK α subunits alone. Currents were activated by voltage steps from −140 mV to +120 mV (20 mV increments) with tail currents at −120 mV. For the three panels below, specific β subunit N-terminal peptides were sequentially applied and washed out from this same patch. ***A2***, 400 μM β3b(1–17) peptide resulted in rapid, incomplete block of BK current, with rapid unblock during the tail currents, an effect similar to the intact β3b subunit (Fig. 1*B*) (Xia et al., 2000). ***A3***, 10 μM β3a(1–20) peptide was applied to the same patch, resulting in slower block, and then a prolonged tail current, characteristic of the intact β3a subunit. ***A4***, 2 μM β2(1–26) peptide was then applied, producing a more complete inactivation of BK current, with little tail current, similar to effects of the intact β2 subunit (Xia et al., 1999). ***B***, Tail currents after the depolarization to +120 mV are shown for control (black circles), β3b peptide (blue line), β2 peptide (green line), and β3a peptide (red line), all from the same patch. ***C***, The integral of current flux during the tail current is plotted as a function of command-step duration for control and peptide conditions. Net current flux in the presence of β3b peptide varies with command-step duration in a manner similar to control currents, indicative that β3b blocked channels rapidly return to a fully open state. For the β2 peptide, net tail current flux is reduced as block develops. For β3a peptide, net tail current flux increases markedly over that expected for all open BK channels simply passing back through a single open state. ***D***, Differences in the effects of β2 and β3a N termini on BK tail currents may arise from different pathways of recovery from inactivation. Arrows highlight possible preferred recovery paths for the two different N termini.

Gomez et al., 2007) in which any such central cavity interloper seems to fully occupy almost all available space. However, recent results with BK channels have raised the possibility that the architecture of the BK central cavity and the entry path to that cavity may be quite distinct from that in Kv channels (Li and Aldrich, 2004, 2006; Wilkens and Aldrich, 2006). Future efforts therefore require new strategies to define the pore architecture of BK channels in resting and open states, along with delineation of specific sites of interaction of N-terminal peptides with the central cavity.

References

Benzinger GR, Xia XM, Lingle CJ (2006) Direct observation of a preinactivated, open state in BK channels with β2 subunits. J Gen Physiol 127:119–131.

Cox D, Aldrich R (2000) Role of the β1 subunit in large-conductance Ca^{2+}-activated K^+ channel gating energetics. Mechanisms of enhanced Ca^{2+} sensitivity. J Gen Physiol 116:411–432.

Demo SD, Yellen G (1991) The inactivation gate of the Shaker K^+ channel behaves like an open-channel blocker. Neuron 7:743–753.

Faber ES, Sah P (2002) Physiological role of calcium-activated potassium currents in the rat lateral amygdala. J Neurosci 22:1618–1628.

Faraldo-Gomez JD, Kutluay E, Jogini V, Zhao Y, Heginbotham L, Roux B (2007) Mechanism of intracellular block of the KcsA K+ channel by tetrabutylammonium: insights from X-ray crystallography, electrophysiology and replica-exchange molecular dynamics simulations. J Mol Biol 365:649–662.

Grieco TM, Malhotra JD, Chen C, Isom LL, Raman IM (2005) Open-channel block by the cytoplasmic tail of sodium channel beta4 as a mechanism for resurgent sodium current. Neuron 45:233–244.

Hille B (2001) Ionic channels of excitable membranes, Ed 3. Sunderland, MA: Sinauer Associates.

Li W, Aldrich RW (2004) Unique inner pore properties of BK channels revealed by quaternary ammonium block. J Gen Physiol 124:43–57.

Li W, Aldrich RW (2006) State-dependent block of BK channels by synthesized shaker ball peptides. J Gen Physiol 128:423–441.

Lingle CJ, Zeng X-H, Ding J-P, Xia X-M (2001) Inactivation of BK channels mediated by the N-terminus of the β3b auxiliary subunit involves a two-step mechanism: possible separation of binding and blockade. J Gen Physiol 117:583–605.

Orio P, Rojas P, Ferreira G, Latorre R (2002) New disguises for an old channel: MaxiK channel beta-subunits. News Physiol Sci 17:156–161.

Raman IM, Bean BP (2001) Inactivation and recovery of sodium currents in cerebellar Purkinje neurons: evidence for two mechanisms. Biophys J 80:729–737.

Shao LR, Halvorsrud R, Borg-Graham L, Storm JF (1999) The role of BK-type Ca^{2+}dependent K^+ channels in spike broadening during repetitive firing in rat hippocampal pyramidal cells. J Physiol (Lond) 521:135–146.

Solaro CR, Prakriya M, Ding JP, Lingle CJ (1995) Inactivating and noninactivating Ca^{2+}-and voltage-dependent K^+ current in rat adrenal chromaffin cells. J Neurosci 15:6110–6123.

Uebele VN, Lagrutta A, Wade T, Figueroa DJ, Liu Y, McKenna E, Austin CP, Bennett PB, Swanson R (2000) Cloning and functional expression of two families of beta-subunits of the large conductance calcium-activated K^+ channel. J Biol Chem 275:23211–23218.

Wallner M, Meera P, Toro L (1999) Molecular basis of fast inactivation in voltage and Ca^{2+}-activated K^+ channels: a transmembrane beta-subunit homolog. Proc Natl Acad Sci USA 96:4137–4142.

Wilkens CM, Aldrich RW (2006) State-independent block of BK channels by an intracellular quaternary ammonium. J Gen Physiol 128:347–364.

Xia XM, Ding JP, Lingle CJ (1999) Molecular basis for the inactivation of Ca^{2+}-and voltage-dependent BK channels in adrenal chromaffin cells and rat insulinoma tumor cells. J Neurosci 19:5255–5264.

Xia XM, Ding JP, Zeng XH, Duan KL, Lingle CJ (2000) Rectification and rapid activation at low Ca^{2+} of Ca^{2+}-activated, voltage-dependent BK currents: consequences of rapid inactivation by a novel β subunit. J Neurosci 20:4890–4903.

Xia XM, Zeng X, Lingle CJ (2002) Multiple regulatory sites in large-conductance calcium-activated potassium channels. Nature 418:880–884.

Zeng XH, Xia XM, Lingle CJ (2003) Redox-sensitive extracellular gates formed by auxiliary beta subunits of calcium-activated potassium channels. Nat Struct Biol 10:448–454.

Zhou M, Morais-Cabral JH, Mann S, MacKinnon R (2001) Potassium channel receptor site for the inactivation gate and quaternary amine inhibitors. Nature 411:657–661.